EXPERIMENTAL INVESTIGATION OF THE COMBINED NATURAL AND FORCED CONVECTION IN AN OPEN ISOTHERMAL CUBIC CAVITY

by

Miloš D. PAVLOVIĆ

Original scientific paper
UDC: 536.331
BIBLID: 0354–9836, *4* (2000), 2, 41–53

The aim of the paper is to examine combined free and forced convection in open isothermal cubic cavity. The experimental apparatus, enabling convective heat transfer coefficient, was particularly designed for this study. Three cavity models were built and tested, varying the surface temperature, the external wind velocity, the angle of incidence and the angle of attack. As a result, a correlation among Nuselt, Grasshof and Reynolds numbers was obtained with high certainty. Using simple visualization technique, fluid field structure is analyzed for different positions and angles of attack of the external flow. In order to study interaction, results obtained by visualization are compared with maps of surface distribution of the local heat transfer coefficient. Conclusions performed enable control of the convective heat transfer process in the cavity, what is important for application in the technical practice.

Introduction

Interaction between fluid and solid body, usually understands mechanical aspect of the problem, *i. e.* to determine force acting on the body. Nevertheless, if there is thermal disequilibrium between fluid and body, on its surface appears thermal interaction, known in science and engineering as convection. For a long period, since convection is studied, interest of the researchers is directed to either natural or forced convection. In the case of natural, free convection, movement of the fluid particles heated on the body generates spontaneously convective flow and heat transfer process. In this case, buoyancy and inertial forces are of same order of magnitude and there is uniform development of velocity and temperature field. Heat transfer process, defined with heat transfer coefficient h, or its dimensionless form Nusselt number Nu, are dependant on Grasshof number Gr, $Nu_n = Nu_n(Gr)$. In the case of forced convection heat transfer process, as well as flow field in the vicinity of the body, are under strong domination of the external flow. Since the only parameter of the external flow is Reynolds number Re, in the case of forced convection heat transfer process can be defined in the form $Nu_f = Nu_f(Re)$. Thermal influence of the body on the external flow is in the case of forced convection is minimal.

Nature of the combined convection phenomenon is complex, since effects of natural and forced development of the velocity and thermal fields are included. That means that in theoretical and experimental analysis of the treated problem exists an equal treatment of both major parameters Grasshof and Reynolds number. In the case of the combined convection heat transfer process is described in the form Nu = Nu(Gr,Re).

In the recent time study of the combined convection attracts attention of researchers, due to its application in technical practice. However, for complex geometry, like open plane or cubic cavity, their efforts are directed mainly to the problem of free convection. Reliable results on natural convective flow and heat transfer process can be found in the papers of Penot et Mirenayat [1], Humphrey *et al.*, [2], Kraabel [3], and Hess et Henze [4]. In the presented paper combined free and forced convection inside an isothermal cubic cavity, open on one side, is treated. Besides the experimental data on heat transfer process, interesting results of convective flow visualization are reported, so that interaction of external forced and internal free convective flow interaction can be analyzed.

Experimental equipment and procedure

Experimental research of the combined free and forced convection was performed in Laboratoire d'étude thermiques, University of Poitiers, France. The experimental rig is a complex system, shown on the Fig. 1, which consists of the cavity model, electronic processor, data acquisition system (DAC) with computer, and low velocity wind tunnel with constant temperature anemometry (CTA) system. In some earlier papers of the author, [5] and [6], experimental installation, as well as experimental procedure, and data treatment were covered in details, so that in this paper they will be reported briefly.

The construction of the cavity was modular, which facilitated realization of different size models. The base of the modular element was duralumin plate,

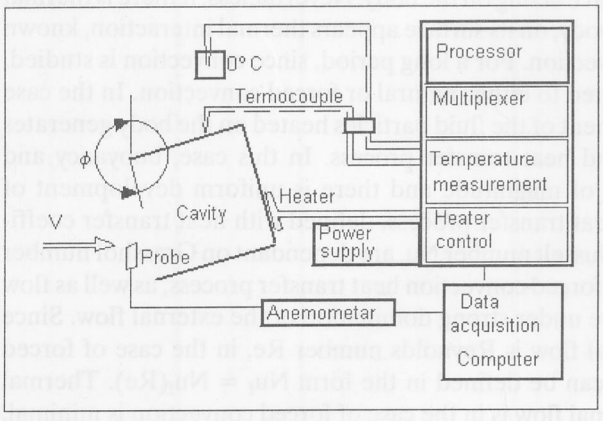

Figure 1. Schematic view of experimental apparatus

200×200×20 mm, with electric heater (70 W), embedded in refractory cement, insulated with two mica slices, and glued on the backside of the element. One Cu-Const thermocouple, inserted in the center of the front side of the element controlled the temperature. Lateral side of the element is profiled in dovetail form, which enables mounting of self-supporting structures. The outer side of the cavity model was well insulated with fiberglass and covered with wooden panels. It was mounted on a metallic support, permitting different orientations of the cavity model with respect to gravity (angle of incidence Φ) and wind direction (angle of attack α). Front face of the model, around the cavity aperture, was a flat plate.

The cavity model was coupled with electronic processor, designed to maintain the surface temperature T_p constant (±0,2 °C), turning corresponding electric heater on/off during each. Uniformity and steadiness of the surface temperature was provided with relatively short duration of scanning cycle (0.5 s). Electric energy dissipated for heating of each element, was transferred by DAC, and registered by the computer.

The cavity model was placed in low velocity wind tunnel. Velocity was measured with CTA system coupled with DAC and computers running the experiment. Hot wire probe was particularly calibrated for extremely low velocity range.

For the described experimental model of the cavity, total heat loss of an element is equal to the electric energy dissipated for its heating. Total heat loss of the modular element i during experiment can be obtained as:

$$q_i = \frac{1}{R_i N t} \sum_{k=1}^{N} L_{ik} U_k^2 t_k; \quad L_{ik} = \begin{cases} 1 \text{ if } T_{ik} < T_p \\ 0 \text{ if } T_{ik} \geq T_p \end{cases} \tag{1}$$

Total heat loss of the cavity, or one of its faces (floor, bottom, ceiling, lateral right and left) is the sum of total heat losses of its elements.

Total heat loss of the cavity (or its faces and elements) consists of convective, q_c, radiative, q_r, and conductive, q_{cd}, ones. So convective heat loss can be determined as:

$$q_c = q - q_r - q_{cd} \tag{2}$$

The radiative heat loss can be calculated as:

$$q_r = \varepsilon \sigma S (T_p^4 - T_a^4) \tag{3}$$

Conductive heat loss was obtained from the trial tests with cavity aperture closed with cover made of the modular elements and kept at the same surface temperature. In this way, only conductive heat loss was measured, since radiative and convective heat ones are eliminated. Tests were done for different surface temperatures T_p, so that empirical correlation for the conductive heat loss was obtained in the form:

$$q_{cd} = a_1 (T_p - T_a)^4 + a_2 (T_p - T_a)^3 + a^3 (T_p - T_a) + a_4 \tag{4}$$

Using the eqs. (2), (1), (3) and (4) convective heat loss of the cavity, or its face or element, can be obtained.

Experimental conditions and results

Experimental conditions

Experimental installation used in this research project permitted certain variations of the experimental conditions. In this way, three cubic cavities of different sizes L : 0.6 m (45 modular elements), 0.4 (20 modular elements) and 0.2 (5 modular elements) were built and tested. The surface temperature was from 300 °C to 1300 °C, and the external flow velocity was from 0.3 m/s to 1.2 m/s. The inclination angle Φ, in vertical plane was varied from 450 to (aperture looking upwards) to 135°. The angle of incidence α, in horizontal plane, was from 90° (aperture normal to the external flow direction) to 90° (aperture parallel to the external flow direction). Larger angles of incidence were not tested since in this case, the aperture of the cavity is in the wake region and results depend mainly of the external shape of the model.

Experimental results

The variation of the basic experimental conditions, quoted above, causes the variation of the convective heat transfer rate of the cavity. In order to generalize both experimental conditions and results, usual dimensionless parameters are involved:

$$\begin{aligned} \mathrm{Gr} &= \frac{g\beta(T_p - T_a)L^3}{\nu^2} = 4.5\cdot 10^7 - 3.5\cdot 10^9 \\ \mathrm{Re} &= \frac{vL}{\nu} = 5.5\cdot 10^3 - 4.5\cdot 10^4 \\ \mathrm{Nu} &= \frac{hL}{\lambda} = \frac{q_d L}{S(T_p - T_a)\lambda} = 40 - 70 \end{aligned} \tag{5}$$

Variations of the dimensionless parameters due to variations of the experimental conditions are given on the right side of the expressions (5). All physical properties of the air (working fluid) are taken at the ambient temperature T_a.

In the treated problem, the hypothesis is posed that natural convection is basic phenomenon of convective flow and heat transfer process. In this way its influence can be separated and general correlation among dimensionless parameters is proposed in the form:

$$\mathrm{Nu} = \mathrm{Nu}_n(\mathrm{Gr},\Phi) f(\mathrm{Re}/\mathrm{Gr}^{1/2},\Phi,\alpha) = a(\Phi)\mathrm{Gr}^{b(\Phi)}\left[1 + c(\Phi,\alpha\left(\frac{\mathrm{Re}}{\mathrm{Gr}^{1/2}}\right)^{d(\Phi,\alpha)}\right] \tag{6}$$

It is important to mention that for the combined convection dimensionless parameter $\mathrm{Re}/\mathrm{Gr}^{1/2}$ is involved. Separating the influence of the natural convection in the eq. (6), it was necessary to determine firstly correlation:

$$\mathrm{Nu}_n(\mathrm{Gr},\Phi) = a(\Phi)\mathrm{Gr}^{b(F)} \tag{7}$$

Therefore, particular series of 84 experiments was performed, for the case of natural convection, in order to obtain values of $a(\Phi)$ and $b(\Phi)$. Afterwards, for the case of the combined convection ten series with 534 experiments were accomplished in order to obtain values of $c(\Phi,\alpha)$ and $d(\Phi,\alpha)$. Results of regressional analysis of experimental date are presented in the Table 1. Very high values of coefficient of correlation testify high certainty of the obtained results.

Table 1. Results of regressional analysis of the experimental data for the cases of natural and combined convection

Φ [°]	a	b	Coef. cor.	α [°]	c	d	Coef. cor.
45	0.047	0.370	0.981	0	0.2710	2.0477	0.966
60	0.048	0.369	0.983	0	0.2733	1.4177	0.868
90	0.093	0.333	0.992	0	0.4771	0.9145	0.978
105	0.080	0.333	0.986	0	0.6693	1.2000	0.952
116	0.065	0.333	0.988	0	0.9931	1.0600	0.992
135	0.060	0.320	0.986	0	1.0036	1.3514	0.992
90			0.992	22.5	0.4903	0.8370	0.976
90			0.992	45	0.5775	0.7570	0.919
90			0.992	67.5	0.5702	0.5858	0.923
90			0.992	90	0.7053	0.8417	0.961

In order to enlarge usefulness of the obtained results in technical practice, further regressional analysis, which define the dependence of the coefficient c and exponent d on angle of incidence Φ and angle of attack α, was done. In this way, empirical correlations in the form of the fourth order polynomials are obtained.

$$\begin{aligned} c(\Phi = 90°, \alpha) &= c_{0\alpha} + c_{1\alpha}\alpha + c_{2\alpha}\alpha^2 + c_{3\alpha}\alpha^3 + c_{4\alpha}\alpha^4, \\ d(\Phi = 90°, \alpha) &= d_{0\alpha} + d_{1\alpha}\alpha + d_{2\alpha}\alpha^2 + d_{3\alpha}\alpha^3 + d_{4\alpha}\alpha^4, \\ c(\Phi, \alpha = 0°) &= c_{0\Phi} + c_{1\Phi}\alpha + c_{2\Phi}\alpha^2 + c_{3\Phi}\alpha^3 + c_{4\Phi}\alpha^4, \\ d(\Phi, \alpha = 0°) &= d_{0\Phi} + d_{1\Phi}\alpha + d_{2\Phi}\alpha^2 + c_{3\Phi}\alpha^3 + c_{4\Phi}\alpha^4, \end{aligned} \tag{8}$$

Results of the regressional analysis for empirical correlations (8) are given in the Table 2.

Usefulness of the proposed correlation (5) for the case of the combined convection is evident from the Figs. 2 and 3. On the Fig. 2 coarse experimental data are presented for the basic position of the cavity ($\Phi = 90°, \alpha = 0°$, cavity aperture vertical and normal to external flow direction). Three groups, for three tested models of the cavity ($L = 0.2$ m,

Table 2. Results of regressional analysis for coefficient *c* and exponent *d*

i	α [°]	$c_{i\alpha}$	ε_c	$d_{i\alpha}$	ε_d	Φ [°]	$c_{i\Phi}$	ε_c	$d_{i\Phi}$	ε_d
0	0	0.4771	.000	0.9145	.000	45	0.2710	.012	2.0477	–.004
1	22.5	0.4903	.000	0.8370	.000	60	0.2773	–.036	1.4177	.016
2	45.0	0.5775	.000	0.7570	.000	90	0.4771	.073	0.9145	–.089
3	67.5	0.5702	.000	0.5958	.000	105	0.6693	–.093	1.2000	.120
4	90.0	0.7053	.000	0.8417	.000	116	0.9931	.039	1.0600	–.084
5						135	1.0036	–.005	1.3514	.008

0.4 m and 0.6 m), each with five series of data, for different Grasshof numbers, marked on the plot, are evident.

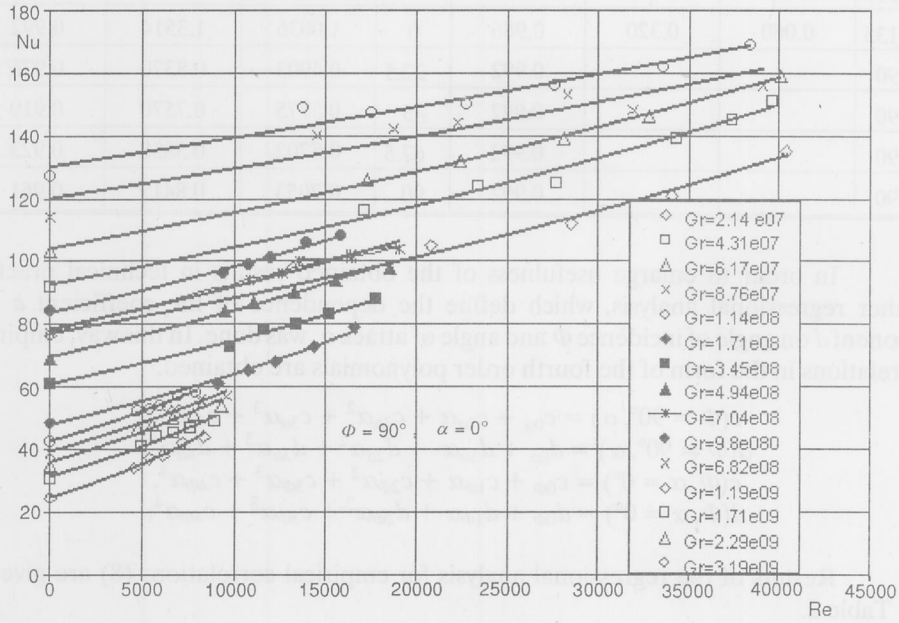

Figure 2. Experimental results for basic position of the cavity ($\Phi = 90°, \alpha = 0°$)
$Gr = 2.14 \cdot 10^7 - 1.14 \cdot 10^8$ – cavity L = 0.2 m;
$Gr = 1.71 \cdot 10^8 - 9.80 \cdot 10^8$ – cavity L = 0.4 m;
$Gr = 6.82 \cdot 10^8 - 3.19 \cdot 10^9$ – cavity L = 0.6 m

On the vertical axis, the values of Nuselt number for natural convection Nu_n are plotted. Using the expression (5) the same experimental results are transformed and expressed as unique data group on the Fig. 3.

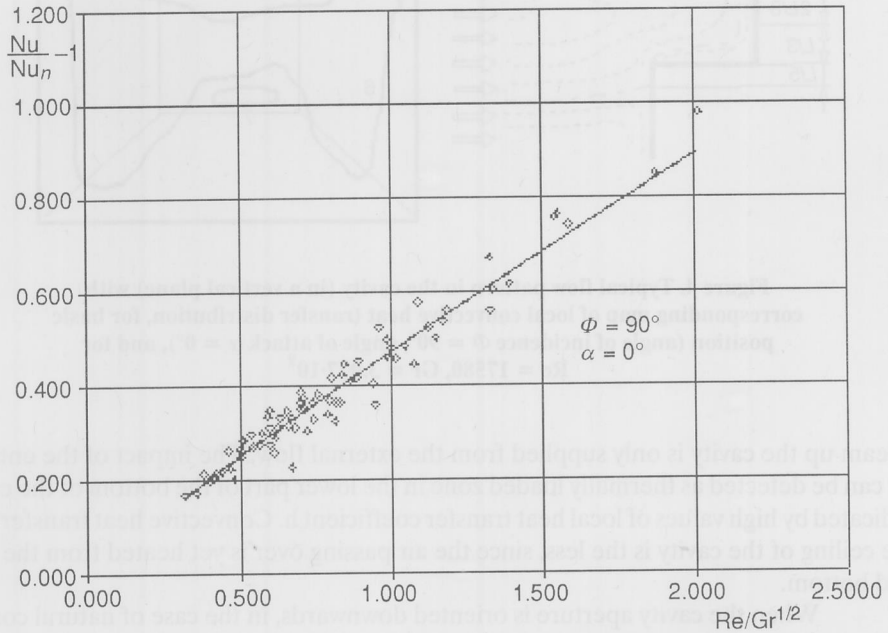

Figure 3. Treated experimental data for basic position of the cavity ($\Phi = 90°, \alpha = 0°$)

Convective flow and heat transfer in the cavity

In order to examine fluid flow structure in the cavity, flow visualization experiments were carried out on the biggest tested model of the cavity ($L = 0.6$ m), involving white smoke in the stream. Due to configuration of the tested model, and three-dimensional character of the flow, it was impossible to take photos, so that flow patterns were sketched. They were completed with maps of the cavity with measured local heat transfer coefficient h distribution. As it was stated in the section 2, convective heat loss was calculated for each particular modular element of the cavity, so that maps of iso-h lines can be obtained by interpolation. In this way, interaction between external forced flow and internal natural convective flow can be better understood.

On the Fig. 4, the results for the basic position ($\Phi = 90°, \alpha = 0°$) are shown. Natural convective flow, from the leading edge of the floor, along the floor, bottom and ceiling of the cavity, and then out, is not greatly affected by the external flow. The main

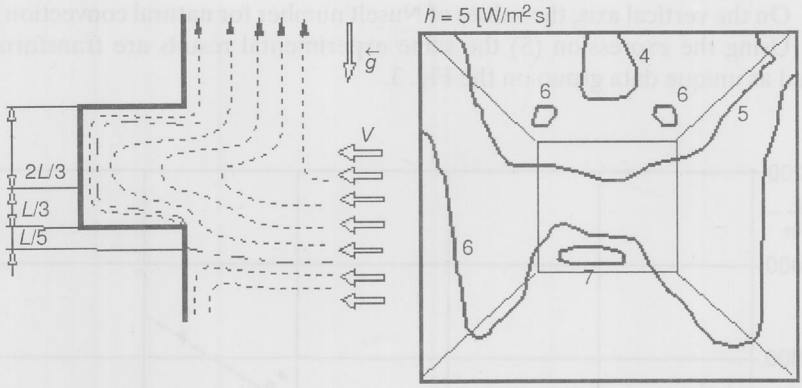

Figure 4. Typical flow pattern in the cavity (in a vertical plane) with corresponding map of local convective heat transfer distribution, for basic position (angle of incidence $\Phi = 90°$, angle of attack $\alpha = 0°$), and for Re = 17580, Gr = $3.077 \cdot 10^9$

stream up the cavity is only supplied from the external flow. The impact of the entering jet can be detected as thermally loaded zone in the lower part of the bottom of the cavity, indicated by high values of local heat transfer coefficient h. Convective heat transfer from the ceiling of the cavity is the less, since the air passing over is yet heated from the floor and bottom.

When the cavity aperture is oriented downwards, in the case of natural convection, there is a stagnation zone in the upper part of the cavity. This position is convenient for reduction of convective hear transfer. In the presence of the external flow, Fig. 5, velocity of the mainstream is higher, provoking vortical motion in the upper part of the cavity, and convective heat transfer is enhanced in comparison with the case of natural convection. Nevertheless, for the same Reynolds number Re, cavity with aperture turned downwards still has importantly less convective heat loss than in the basic position (vertical aperture). Low convective heat transfer zones are obvious on the corresponding map of the cavity.

The case shown on the Fig. 6, when the cavity aperture is oriented upwards, is very interesting explaining correspondent results of regressional analysis. The vortical motion about horizontal axis, formed in the lower part of the cavity by viscous effects of the mainstream, becomes unstable since it is affected by buoyancy driven natural convective motion. This explains lower values of the coefficients of correlation (Table 1) for these cases. In this position, convective heat transfer is enhanced in comparison with the basic position of the cavity.

Turning the cavity about vertical axis changes the angle of attack α in horizontal plane. In this case, one lateral place becomes partially hidden, and the other exposed to the external flow. For angles of attack $\alpha < 30°$ growth of the thermal boundary layer on the hidden lateral face can be noticed, as well as growth of the external velocity for the

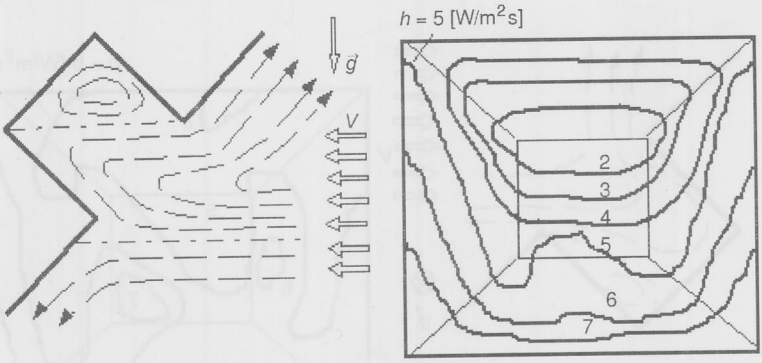

Figure 5. Typical flow pattern in the cavity (in a vertical plane) with corresponding map of local convective heat transfer distribution. Cavity aperture is turned downwards (angle of incidence Φ = 135°, angle of attack α = 0°), the map is for Re = 39460, Gr = $1.815 \cdot 10^9$

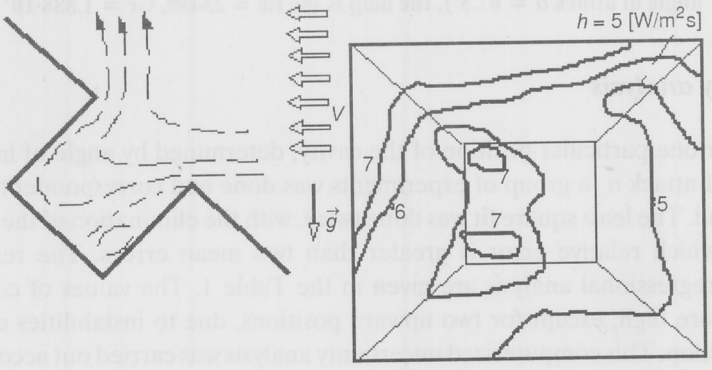

Figure 6. Typical flow pattern in the cavity (in a vertical plane) with corresponding map of local convective heat transfer distribution. Cavity aperture is turned upwards (angle of incidence Φ = 45°, angle of attack α = 0°), the map is for Re = 39560, Gr = $1.732 \cdot 10^9$

boundary layer on the exposed face. In comparison with the basic position ($\Phi = 90°, \alpha = 0°$) convective heat transfer is enhanced on both lateral faces. For angles of attack $\alpha > 30°$, separation of the boundary layer on a hidden face occurs, and vertical vortical structure is formed in the zone of separation, Fig 7. It is very well illustrated by the region of high heat transfer coefficient, in the form of strip, on the hidden lateral face. It is also evident that the influence of the entering jet is turned towards the exposed lateral face. Comparing the position of the cavity with certain angle of attack $\alpha > 0°$, with the basic position ($\Phi = 90°$, $\alpha = 0°$), it seems that the convective heat transfer for entire cavity is importantly enhanced.

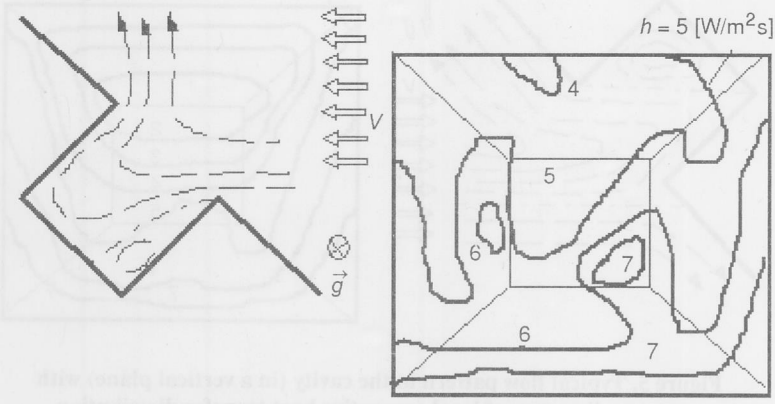

Figure 7. Typical flow pattern in the cavity (in a horizontal plane) with corresponding map of local convective heat transfer distribution. Cavity aperture is turned sideways (angle of incidence $\Phi = 90°$, angle of attack $\alpha = 67.5°$), the map is for Re = 23450, Gr = $1.888 \cdot 10^9$

Uncertainty analysis

For one particular position of the cavity, determined by angle of inclination Φ and angle of attack α, a group of experiments was done and correspondent correlation (9) was found. The least square fit was done twice, with the elimination of the experimental results which relative error is greater than two mean errors. The results of the performed regressional analysis are given in the Table 1. The values of coefficient of correlation are high, except for two upward positions, due to instabilities explained in previous section. This computerized uncertainty analysis was carried out according to the procedure described by Moffat [7].

The systematic error of the applied experimental apparatus and procedure, according to eqs. (6) and (5), and using eqs. (1–4) can be assumed as:

$$\frac{\Delta \mathrm{Nu}}{\mathrm{Nu}} = \frac{\Delta T_p + \Delta T_a}{T_p - T_a} + \frac{\Delta q}{q} + \frac{\Delta q_r}{q_r} + \frac{\Delta q_{cd}}{q_{cd}} = 0.005 + 0.09\frac{q_{cd}}{q_c} + 0.18\frac{q_r}{q_c} \qquad (9)$$

In the expression (9) the ratios q_{cd}/q_c and q_r/q_c depend on $\mathrm{Re}/\mathrm{Gr}^{1/2}$ and α. Assuming the particular experimental results obtained for the conductive q_{cd}, radiative q_r and convective heat losses q_c, the systematic error can be evaluated to range between 7.5 and 14%. It is evidently smaller than in the case of the natural convection, [1] and [2], since the convective heat losses measured for the natural convection are smaller in comparison with mixed convection, while conductive and radiative ones are almost the same.

Practical significance of the presented study

The experimental results obtained in presented study are very important for application in technical practice. The convective heat loss of different technical objects in the form of cubic cavity can be predicted using correlations (6) and (7). The usefulness of the proposed procedure can be demonstrated by the central solar receiver for French power plant THEMIS (10 MWs). The receiver is in the form of cubic cavity (L = 4 m), placed on an 80 m high tower, and oriented downwards (Φ = 1200), in order to collect solar energy from 200 plane heliostats of 50 m^2. The working surface temperature of the receiver is T_p = 400 °C, which gives for the air as a working fluid Grasshof number Gr = $= 3.5 \cdot 10^{12}$.

Working in the natural convective regime, without wind, corresponding Nuselt number is Nu_n = 792, which gives convective heat loss of 139 kW (P_c/P_e = 5.6%). Presence of the external wind importantly amplifies convective heat losses of the receiver. For the wind velocity of v = 7m/s, that gives Re = $1.79 \cdot 10^6$, Nuselt number is Nu = 1564, and corresponding convective heat loss is 275 kW (P_c/P_e = 11%) – almost double in comparison with the absence of wind. Usually, estimation of receiver heat losses presumes the natural convective and neglects the influence of the external wind. This simple example proves that for central solar receivers model of combined convection regime is more correct and convenient.

Conclusion

In this paper, the results of experimental study of combined natural and forced convection in an open isothermal cubic cavity are presented. Particularly designed experimental apparatus, with three cavity models of different sizes, was used to provide a large experimental database. Performed regressional analysis of the experimental results gives correlation among Nuselt, Grasshof and Reynolds number for the cavity. In comparison with corresponding studies of the natural convection, estimated systematic error is less. For different technical objects in the form of open cavity, estimation of the convective heat losses can be easily done using obtained results.

Particular contributions of the presented study are the results of fluid flow visualization, completed with the maps of the cavity with measured local heat transfer coefficient h distribution. In this way, for different typical positions of the cavity, interaction between external forced flow and internal natural convective flow, as well as resulting convective heat transfer can be better understand.

In the former studies of the convective heat transfer in the open cavity, particularly for high Grasshof numbers, problem was treated as natural convection, assuming that it cannot be greatly affected by the external flow. Presented experimental study clearly confirms considerable influence of the external flow on the convective heat transfer phenomenon, and provides reliable procedure for its estimation.

Nomenclature

a_i $i = 1, 2, ...4$ – coefficients in eq. (4)
a – coefficient in eq. (7), dimensionless
b – exponent in eq. (7), dimensionless
c – coefficient in eq. (6), dimensionless
$c_{i\alpha}$ $i = 0, 1, ...4$ – coefficient in eq. (8), dimensionless
$d_{i\alpha}$ $i = 0, 1, ...4$ – coefficient in eq. (8), dimensionless
d – exponent in eq. (6), dimensionless
$c_{i\Phi}$ $i = 0, 1, ...4$ – coefficient in eq. (8), dimensionless
$d_{i\Phi}$ $i = 0, 1, ...4$ – coefficient in eq. (8), dimensionless
g [ms^{-1}] – local gravitational acceleration
Gr – Grasshof number, eq. (5), dimensionless
h [Wm^{2}s^{-1}] – heat transfer coefficient
L [m] – length of the cavity
L_{ik} – heating command, dimensionless
N – total number of cycles during one experiment, dimensionless
Nu – Nusselt number, eq. (5), dimensionless
Nu_n – Nusselt number for natural convection, dimensionless
q [W] – total heat loss, eq. (1)
q_c [W] – convective heat loss, eq. (2)
q_r [W] – radiative heat loss, eq. (3)
q_{cd} [W] – conductive heat loss, eq. (4)
R [Ω] – electric resistance
Re – Reynolds number, eq. (5), dimensionless
S [m^2] – surface area of the cavity
T [K] – temperature
T_a [K] – ambient temperature
T_p [K] – surface temperature
t [s] – duration of the scanning cycle
U [V] – electric voltage
v [ms^{-1}] – velocity

Greek symbols

α – angle of incidence
Φ – angle of inclination
β [K^{-1}] – cubic expansion coefficient
Δ – solute error, difference
ε – emissivity, dimensionless
λ [Wm^{-1} K^{-1}] – thermal conductivity
ν [m^{2}s^{-1}] – kinematic viscosity

Subscripts

i=1,2,...m – index of a modular element
k=1,2,...N – index of a scanning cycle

References

[1] Mirenayat, H., Etude expérimental du transfert de chaleur par convection naturelle dans une cavité isotherme ouverte, Thèse de Docteur-Ingenieur, Université de Poitiers, France, 1981
[2] Humphrey, J. A. C., Sherman, F. S., Chen, K. S., Experimental Study of Free and Mixed Convective Flow of Air in a Heated Cavity, Rep. No 83-1, University of California, Berkeley, USA, 1983

[3] Kraabel, J. S., An Experimental Investigation of the Natural Convection from a Side-Facing Cubical Cavity, ASME-JSME Thermal Eng. Joint Conf., 1983, Honolulu, USA, pp. 299–306
[4] Hess, C. F., Henze, R. H., Experimental Investigation of Natural Convection Losses from Open Cavities, *Journal of Heat Transfer, 106* (1984), pp. 333–338
[5] Pavlović, M. D., Correlation Between the Flow Field Structure and the Heat Transfer in an Open Isothermal Cubic Cavity, *ZAMM, 69* (1989) 6, pp. 646–647
[6] Pavlović, M. D., Penot, F., Experiment in the Mixed Convection Regime in an Isothermal Open Cubic Cavity, *Journal of Experimental Thermal and Fluid Science, 4* (1991), pp. 648–655
[7] Moffat, R. J., Describing the Uncertainties in Experimental Results, *Journal of Experimental Thermal and Fluid Science, 1* (1988), pp. 3–17

Author's address:

M. D. Pavlović
Chair for Fluid Mechanics,
Faculty of Mechanical Engineering, University of Belgrade
80, 27. marta, 11000 Belgrade, Yugoslavia
Tel. (381)(11)33-70-371, e-mail: milpav@alfa.mas.bg.ac.yu

Paper submited: April 20, 2001
Paper revised: October 5, 2001
Paper accepted: November 7, 2001